



Cite this: *Dalton Trans.*, 2025, **54**, 8385

Recent advances and challenges of metal–organic frameworks for CO₂ capture

Runzhi Wei,^a Tao Zhao,^a Hui Xu^{*b} and Junkuo Gao ^{*a}

Carbon dioxide (CO₂) emissions resulting from extensive fossil fuel consumption have become an increasingly critical global challenge, underscoring the importance of carbon capture and separation technologies. As emerging porous materials, metal–organic frameworks (MOFs) exhibit remarkable potential for CO₂ capture due to their unique structures and tunable properties. Current MOF-based CO₂ capture methods have been broadly categorized into two major mechanisms: chemisorption and physisorption. By precisely tailoring MOF pore size and shape, creating unsaturated metal sites, and introducing functional groups, researchers significantly boost CO₂ capture efficiency. This Frontier article discussed these two mechanisms and highlighted the latest advances in MOF-based CO₂ capture, offering valuable guidelines for the development of novel MOF-related technologies.

Received 25th January 2025,
Accepted 25th April 2025

DOI: 10.1039/d5dt00204d

rs.c.li/dalton

Introduction

As industrialization progresses, CO₂ emissions continue to rise, posing significant risks of global warming that threaten both ecosystems and economies. Hence, the development of effective, low-cost CO₂ capture and storage technologies has become essential for climate action and sustainability.^{1,2} Various carbon capture strategies have been explored. For instance, chemisorption often employs alkaline solutions, but it requires large reagent volumes and additional processing.³

Membrane separation relies on gas permeation through specialized materials, yet producing efficient membranes can be costly.⁴ Cryogenic separation involves liquefying CO₂ at low temperatures, an energy-intensive process requiring complex equipment.⁵ Traditional physisorption utilizes activated carbon and zeolites but would benefit from enhanced selectivity and capacity.⁶

MOFs offer considerable advantages for CO₂ capture. These frameworks, formed by the self-assembly of metal ions or clusters with organic ligands, possess exceptional porosity, high surface area, and tunable pore sizes, making them highly effective adsorbents for CO₂.^{7–9} Compared with other techniques, MOFs often exhibit superior selectivity and capacity for CO₂, aided by customizable pore structures that facilitate targeted uptake. MOF-based CO₂ capture can be categorized

^aSchool of Materials Science and Engineering, Zhejiang Sci-Tech University, Hangzhou 310018, China. E-mail: jkgao@zstu.edu.cn

^bInstitute of Optoelectronic Materials and Devices, China Jiliang University, Hangzhou 310018, China. E-mail: huixu@cjlu.edu.cn



Runzhi Wei

Runzhi Wei obtained her Master's degree from Guilin University of Technology in 2022. She is currently studying at Zhejiang Sci-Tech University under the guidance of Professor Junkuo Gao. Her research mainly focuses on functional porous materials for gas separation.



Tao Zhao

Tao Zhao has been a postgraduate student at Zhejiang Sci-Tech University (with Professor Junkuo Gao) since September 2022. His main research is on the preparation of MOF and their gas adsorption-separation research.

into chemisorption and physisorption.¹⁰ Chemisorption involves active functional groups or unsaturated metal sites in the MOFs that chemically interact with CO₂ molecules, forming stable bonds and thus enhancing both selectivity and capacity.¹¹ Conversely, physisorption mainly relies on weak interactions (e.g., van der Waals forces, hydrogen bonding, and electrostatic interactions) through the MOFs' high porosity and large surface area.¹² In addition, the molecular sieving effect exploits precisely defined pore apertures to separate gas molecules of varying sizes, further boosting CO₂ capture performance.

In this Frontier article, we surveyed recent progress in the use of MOFs for CO₂ capture. We reviewed two key adsorption mechanisms—chemisorption and physisorption—and discussed their respective advantages and limitations in the context of CO₂ adsorption. Finally, we provided concluding remarks and highlighted future challenges and possible directions for further advancing MOF-based CO₂ capture.

Chemisorption of CO₂ by MOFs

Chemisorption involves the formation of stable chemical bonds often through electron transfer—between MOF components and CO₂.^{13,14} These chemical bonds improve selectivity, which is especially useful for CO₂ capture at low pressures. Strategies to enhance MOF–CO₂ interactions include introducing unsaturated metal sites (UMS) and polar amino groups to optimize MOF performance for carbon capture.^{15–17}

UMS carry a partial positive charge, they exhibit a stronger quadrupole moment and greater polarizability for CO₂ than for nitrogen (N₂).¹⁸ Zhao's group synthesized three MOFs engineered with unsaturated metal sites and nitrogen-dense functional groups, which synergistically improved CO₂ chemisorption efficiency.¹⁹ Among these materials, NTU-113 ([Cu₂(L₃)]_n–1, H₄L₃ = 5,5'-(benzene-1,3-diyl)di-(1*H*-1,2,3-triazole-1,4-diyl)diisophthalic acid) exhibited optimal performance, achieving a CO₂ adsorption capacity of 166.8 cm³ g^{–1}.

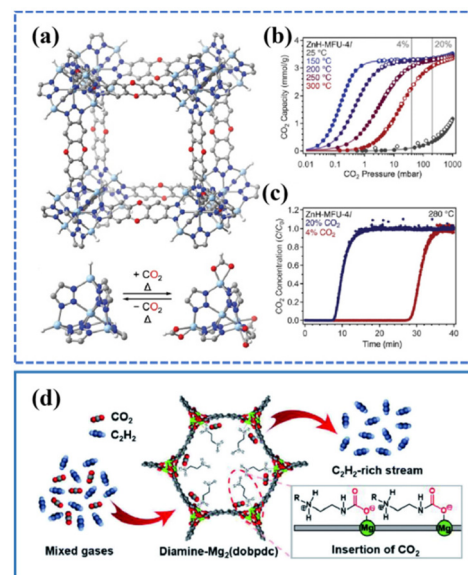


Fig. 1 (a) Structural diagram of ZnH-MFU-4l; (b) variable temperature CO₂ adsorption isotherm of ZnH-MFU-4l; (c) breakthrough data of ZnH-MFU-4l exposed to an airflow of approximately 280 °C. Adapted with permission from ref. 20. Copyright 2024, American Association for the Advancement of Science. (d) Representative structure of diamine-Mg₂(dobpdc) and CO₂ adsorption mechanism. Adapted with permission from ref. 25. Copyright 2021, Royal Society of Chemistry.

More recently, Rohde *et al.*, prepared ZnH-MFU-4l ([Zn₅H_{3.76}Cl_{0.24}(btdd)₃], H₂btdd = bis(1*H*-1,2,3-triazolo[4,5-*b*], [4',5'-*i*])dibenzo [1,4] dioxin), which reversibly captures CO₂ at 200–400 °C.²⁰ Upon CO₂ activation, zinc–hydrogen bonds dissociate to form hydroxyl groups and a stable bond with zinc (Fig. 1(a)). The CO₂ adsorption capacity of ZnH-MFU-4l initially rises with temperature and then stabilizes (Fig. 1(b)). Notably, when exposed to flowing gas with 20% or 4% CO₂, breakthrough occurred rapidly within 10 and 30 minutes, respectively, achieving over 90% capture efficiency in both



Hui Xu

Hui Xu is an Associate Professor at China Jiliang University, China. She received her BS (2008) degree and PhD (2013) from Zhejiang University in China. Her research interest is related to metal–organic frameworks (MOFs) and hydrogen-bonded organic frameworks (HOFs) for gas separation and sensing.



Junkuo Gao

Junkuo Gao is now a Qianjiang Scholar Distinguished Professor at Zhejiang Sci-Tech University, China. He received his BS (2005) degree and PhD (2010) from Zhejiang University in China. He worked at Royal Institute of Technology (KTH), Sweden and at Nanyang Technological University, Singapore as a post-doctoral fellow during 2010–2013. His research interest is related to functional porous materials including metal–organic frameworks (MOFs) and hydrogen-bonded organic frameworks (HOFs) for photo/electrocatalysis and gas separation.

cases (Fig. 1(c)). By directly capturing high-temperature flue gas, ZnH-MFU-4l reduces energy consumption, demonstrating promising potential for future MOF-based CO₂ capture applications.

Besides use of UMS, another effective strategy for CO₂ chemisorption involves the functionalizing MOFs.^{21,22} Amine-based adsorbents are commonly used in large-scale processes to capture carbon dioxide; however, they often generate significant pollution and require substantial energy, prompting the need for more efficient alternatives.²³ By incorporating polar amino groups into MOFs, these groups can form specific chemical bonds with CO₂, thereby improving adsorption efficacy. Zou's group designed a series of amine-functionalized, stable titanium-based MOFs (named MIP-207-NH₂-*n*) by adjusting the ratio of 1,3,5-benzenetricarboxylic acid (H₃BTC) to 5-aminoisophthalic acid (5-NH₂-H₂IPA).²⁴ These MOFs retain the original MIP-207 framework. The addition of amino (-NH₂) groups increased the specific surface area and Lewis basic sites, which improves CO₂ affinity. Choi *et al.* prepared a new MOFs, diamine-Mg₂(dobptc) (H₄dobptc = 4,4'-dioxido-3,3'-biphenyldicarboxylate). This MOFs exhibited strong acid-base interactions with CO₂, which enhanced its specific CO₂ capture capability, achieving a capacity of 3.58–3.82 mmol g⁻¹ at 298 K and 30 mbar (Fig. 1(d)).²⁵

However, in practical industrial applications, the presence of water vapor is inevitable, and its impact on the performance of MOFs exhibits dual characteristics. On one hand, water vapor may induce hydrolysis of the MOF skeleton and compete with carbon dioxide for adsorption sites, thereby reducing the material's adsorption efficiency.²⁶ To address this challenge, Hong's group protected the diamine groups in een-Mg₂(dobpdc) (een = *N*-ethylethylenediamine), with hydrophobic carbonate compounds, such as *tert*-butyl dicarbonate (Boc).²⁷ Boc reacted with the diamines at the pore openings, forming dense hydrophobic amines that prevented moisture entry. The Boc-protected een-MOF-Boc1 showed excellent CO₂ adsorption, even under simulated flue gas with 10% H₂O. On the other hand, the presence of water vapor can, in certain cases, promote the reaction between amino groups and carbon dioxide. Meanwhile, it can improve the utilization efficiency of amino groups and drive the reaction towards the formation of bicarbonate, thereby enhancing the material's carbon dioxide capture ability. Yaghi *et al.*²⁸ developed the polyamine-functionalized

MOF-808-Pas ([Zr₆O₄(OH)₄(BTC)₂(PA)_{*N*}(EtCl)_{3.21-*N*}(OH)_{2.79}(H₂O)_{2.79}], H₃BTC = enzene-1,3,5-tricarboxylic acid, PA = polyamine, EtCl = 3-chloropropionic acid anion). Under the condition of 50% relative humidity, the carbon dioxide absorption reached 1.205 mmol g⁻¹, which was 97% higher than that under dry conditions. In addition, their group also prepared MOF-808-Gly ([Zr₆O₄(OH)₄(BTC)₂(Gly)_{*N*}(OH)_{6-*N*}(H₂O)_{6-*N*}], Gly = glycine) and MOF-808-DL-Lys ([Zr₆O₄(OH)₄(BTC)₂(Lys)_{*N*}(OH)_{6-*N*}(H₂O)_{6-*N*}], Lys = lysine) through the amino-acid functionalization of MOF-808 ([Zr₆O₄(OH)₄(BTC)₂]).²⁹ These materials achieved efficient carbon dioxide capture under flue gas conditions (15% CO₂, 20% RH), with a working capacity of 0.42 mmol

g⁻¹. They could also undergo 80 stable cycles without performance degradation. In contrast, MOF-808-Gly utilizing vacuum swing adsorption (VSA) achieved a regeneration energy demand of approximately 0.5 MJ mol⁻¹ CO₂, which was 6 to 10 times lower than conventional amine systems that required 3 to 5 MJ mol⁻¹. This significant advancement was attributed to the weak physisorption of bicarbonate intermediates, allowing for room-temperature mechanical vacuum desorption rather than energy-intensive thermal processes. These innovations not only tackled the high regeneration costs associated with amine scrubbing but also eliminated the need for high-temperature operations through VSA, thereby offering a practical CO₂ capture solution with improved economic and environmental viability.

Chemisorption achieves strong CO₂ binding through the formation of chemical bonds, resulting in high selectivity, capacity, and stability. This process is particularly effective in high-temperature, high-pressure, and high-CO₂ environments, such as coal-fired flue gas capture and medium to high-pressure natural gas decarbonization. The formation of stable bonds, such as carbamate, between CO₂ and the active sites of the material prolongs breakthrough time and mitigates moisture interference. However, the regeneration process necessitates high temperatures (100–200 °C), which increases energy costs, and amine-functionalized groups may degrade over multiple cycles. Consequently, material design-incorporating unsaturated metal sites and amine grafting-is crucial for balancing adsorption performance with regeneration efficiency to ensure industrial viability.

Physisorption of CO₂ by MOFs

Physisorption does not involve chemical reactions or bond formation. Key characteristics include low heat release, rapid adsorption rates, and generally reversible behavior.³⁰ The high efficiency of physisorption is attributed to the high porosity and large specific surface area of MOFs, which provide abundant adsorption sites. These sites facilitate the binding of CO₂ molecules *via* weak interactions such as hydrogen bonding, electrostatic interactions, and van der Waals forces.³¹

Singh *et al.* developed IISERP-MOF28 ([Zn₂(CH₃COO)(C₂N₄H₃)₂(OH⁻)(H₂O)_{*x*}]), an ultra-microporous MOF (~5 Å pores), which selectively adsorbs CO₂ through its pore structure. Grand Canonical Monte Carlo (GCMC) simulations showed that CO₂ molecules formed hydrogen bonds with hydroxyl groups through their oxygen atoms, while their central carbon atoms engaged in Lewis acid-base interactions with the oxygen atoms of the acetate ligands. This dual synergistic effect significantly enhanced localized adsorption and stabilization within the MOF channels, enhancing adsorption efficiency.³² Functional groups, such as methyl groups, can further tune pore size and enhance CO₂ capture.³³ Yang's group employed a solvothermal method utilizing Al(NO₃)₃·9H₂O, formic acid, and 4,4',4''-(2,4,6-trimethylbenzene-1,3,5-triyl)tribenzoic acid to synthesize a stable aluminum-

based MOF, designated ZJU-620 (Al). This material exhibited a high surface area of $1347 \text{ m}^2 \text{ g}^{-1}$ and a CO_2 adsorption capacity of 4.25 mmol g^{-1} (Fig. 2(b)).³⁴ GCMC simulations revealed two distinct adsorption sites, with site II exhibiting reduced sensitivity to humidity due to the presence of hydrophobic groups. CO_2 interacted strongly with ZJU-620 (Al) through $\text{C}=\text{O} \cdots \text{H}$ interactions (Fig. 2(a)), underscoring its promising potential for CO_2 capture in high-humidity environments (Fig. 2(c)).

Similarly, CALF-20 ($[\text{Zn}_2(1,2,4\text{-triazolate})_2(\text{oxalate})]$), is recognized as one of the most typical carbon dioxide physical adsorbents.³⁵ It featured zinc(II) ions bridged by triazolium and supported by oxalate.³⁶ GCMC simulations showed close CO_2 -triazole interactions, bound by van der Waals forces. CALF-20 adsorbed $4.07 \text{ mmol g}^{-1} \text{ CO}_2$ at 1.2 bar, 293 K, with a CO_2/N_2 selectivity of 230. In addition, recent research increasingly focused on using fluorine-containing anion columns as interlayer supports for constructing MOFs. CO_2 capture was facilitated by electrostatic interactions between electronegative fluorine (F) atoms and carbocation ions.³⁷ Zhang's group reported TIFSIX-Cu-TPA ($[\text{C}_{20}\text{H}_{16}\text{CuF}_6\text{N}_{5.33}\text{Ti}]$), a novel anion pillar material composed of tri(pyridin-4-yl)amine, copper salt, and TiF_6^{2-} .³⁸ This material featured two distinct cage sizes for CO_2 adsorption: smaller cages designed for selectivity and larger cages aimed at enhancing capacity (Fig. 2(d) and (e)). It demonstrated a high CO_2 capacity ranging from 51.7 to $105.4 \text{ cm}^3 \text{ g}^{-1}$, with thermal stability up to 308°C (Fig. 2(f)).

Moreover, molecular sieving technology has been widely recognized as an efficient physical adsorption method. By capitalizing on the inherent pore size characteristics of MOFs, this approach achieves selective gas separation through geometric exclusion mechanisms. Specifically, the engineered pore structures are precisely tailored to be slightly larger than CO_2 molecules (3.3 \AA) while smaller than other gaseous components

such as N_2 (3.64 \AA) and CH_4 (3.8 \AA).³⁹ When gas mixtures flow through these MOF materials, only CO_2 molecules can penetrate the pores and become adsorbed, enabling high-efficiency separation. This technology offers multiple advantages including cost-effectiveness, operational simplicity, recyclable adsorbents, and low energy consumption, making it particularly suitable for large-scale CO_2 capture and storage in industrial applications.⁴⁰ In practical applications, precise control of MOFs pore sizes is crucial for efficient CO_2 capture. Han's group developed In-MOFs with tailored pore sizes ($5\text{--}8.0 \text{ \AA}$) by controlling interpenetration.⁴¹ Dasgupta's group synthesized two stable Zr-MOFs, MOF-808@N ($[\text{Zr}_6\text{O}_6(\text{OH})_4(\text{BTC})_2(\text{CH}_3\text{COO})_6]$, H_3BTC = benzene-1,3,5-tricarboxylic acid) and DUT-67@N ($[\text{Zr}_6\text{O}_4(\text{OH})_4(\text{TDC})_4(\text{CH}_3\text{COO})_4]$, H_2TDC = 2,5-thiophenedicarboxylic acid), with pore sizes of 16 \AA and 12 \AA , respectively.⁴² Due to the smaller size of CO_2 compared to CH_4 , CO_2 molecules entered MOF pores more easily, resulting in high adsorption capacities of 1.3 mmol g^{-1} for MOF-808@N and 1.28 mmol g^{-1} for DUT-67@N at 298 K and 1 bar . Notably, the precise control of pore size enables complete molecular sieving.⁴³ Additionally, Chen's group investigated Cu-F-pymo ($[\text{Cu}(\text{F-pymo})_2(\text{H}_2\text{O})_{1.25}]_n$, F-pymo = 5-fluoropyrimidine-2-olate), an ultramicroporous MOFs of copper(II) and 5-fluoropyrimidine-2-olate, for the separation of CO_2 from CH_4 and N_2 .⁴⁴ The framework's small pore size (3.3 \AA) facilitated CO_2 diffusion while effectively excluding other gases (Fig. 3). The presence of oxygen moieties on its surface enhanced CO_2 binding through electrostatic and hydrogen bonding interactions. At 298 K and 1 bar , Cu-F-pymo exhibited an adsorption capacity of $69.2 \text{ cm}^3 \text{ cm}^{-3}$.

However, in molecular sieving-based gas separation, the primary limitation stems from slow gas diffusion in microporous structures ($<2 \text{ nm}$).⁴⁵ While these frameworks offer high surface area and selective adsorption sites, their narrow pores create diffusion bottlenecks *via* intensified molecule-wall interactions (*e.g.*, van der Waals forces) and thermal gradients from exothermic adsorption, which reduce diffusivity and increase local temperatures.⁴⁶ Collectively, these effects prolong adsorption-desorption cycles and diminish separation efficiency under dynamic conditions. To address diffusion challenges in MOFs, hierarchical pore engineering enhances large-scale CO_2 capture.⁴⁷ Zhao *et al.* recently synthesized

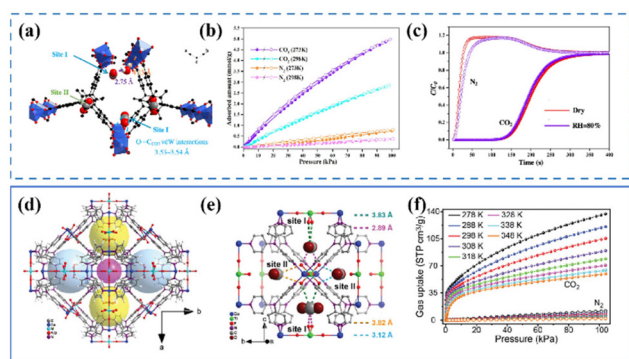


Fig. 2 (a) Binding sites of two CO_2 molecules on ZJU-620(Al); (b) adsorption-desorption isotherms of CO_2 and N_2 by ZJU-620(Al) at 273 and 298 K ; (c) experimental CO_2/N_2 (15/85) dynamic adsorption curves on ZJU-620(Al) under dry & $80\% \text{ RH}$ (b). Adapted with permission from ref. 34. Copyright 2023, American Chemical Society. (d) Overview of an A-Cu-TPA structure; (e) single crystal structure of CO_2 loaded TIFSIX-Cu-TPA; (f) CO_2 and N_2 adsorption isotherms of TIFSIX-Cu-TPA from 278 to 348 K . Adapted with permission from ref. 38. Copyright 2023, Wiley.

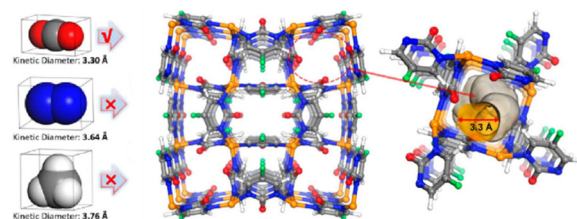


Fig. 3 Illustration of the packing of CO_2 -loaded Cu-F-pymo from GCMC simulations and a schematic of size/shape sieving for CO_2 , N_2 , and CH_4 based on their molecular diameters. Adapted with permission from ref. 44. Copyright 2022, Elsevier.

uniform rht-topology hierarchical MOFs *via* click chemistry using triazole-functionalized dendritic hexacarboxylate ligands and Zn^{2+} ions.⁴⁸ Systematic organic backbone extension yielded tunable pore sizes (13.0–25.0 Å), creating networks that boost CO_2 diffusion while excluding larger molecules. Triazole groups enhance CO_2 binding through electrostatic interactions, validated by gas adsorption showing high porosity. For example, NTU-163 ($[\text{Zn}_3(\text{L}_3)(\text{H}_2\text{O})_3]_n$, $\text{H}_6\text{L}_3 = 5,5',5''\text{-(4,4',4''-((1,3,5-triphenylbenzene)-4,4',4''-triyl)tris(1H-1,2,3-triazole-4,1-diyl))trisisophthalic acid}$) exhibits a BET surface area of $4814 \text{ m}^2 \text{ g}^{-1}$. This design strategy improves carbon capture efficiency, positioning these MOFs as promising candidates for energy-efficient CO_2 separation processes.

Physisorption relies on weak van der Waals forces for reversible CO_2 capture, operating efficiently under low-concentration, low-temperature, and low-to-moderate pressure conditions-ideal for direct air capture (DAC) and natural gas purification. However, its dependence on microporous structures (<2 nm) introduces critical limitations: intensified molecule-wall interactions slow gas diffusion, while exothermic adsorption creates thermal gradients that further hinder mass transport, prolonging cycles. Though low energy consumption aligns with sustainability goals, rapid breakthrough times due to weak binding require frequent regeneration, destabilizing continuous operations. These challenges necessitate pore size optimization and operational parameter tuning to enhance scalability in practical applications.

Conclusions, challenges and future directions

MOFs, with their distinctive pore architectures and tunable dimensions, showed significant promise for CO_2 capture. The capture mechanisms included chemisorption and physisorption.

Chemisorption, which utilizes the binding forces of chemical bonds, offers significant advantages such as high capacity, selectivity, and stability in environments characterized by high temperatures, pressures, and concentrations of CO_2 (e.g., in coal-fired flue gas and natural gas capture). This makes it particularly effective for efficient capture at low pressures. Furthermore, the integration of these materials with membrane separation technologies can enhance selectivity. However, practical applications encounter several challenges: competitive adsorption between water molecules and CO_2 for active sites reduces capture efficiency; the degradation of amine-based functional groups and difficulties in regeneration limit cycling stability; and the extended breakthrough time coupled with high energy consumption associated with temperature/pressure swing regeneration processes complicates industrial scalability.

Physisorption, which utilizes weak van der Waals forces for reversible CO_2 capture, presents several advantages, including low energy consumption and operational feasibility under conditions of low concentration, low temperature, and low to mod-

erate pressure. It is particularly suitable for applications such as DAC and natural gas purification. However, its dependence on microporous architectures (with pore sizes <2 nm) introduces significant challenges: intensified interactions between molecules and pore walls impede gas diffusion kinetics, while exothermic adsorption-induced thermal gradients further exacerbate mass transport limitations, collectively extending the durations of adsorption-desorption cycles. Moreover, the inherently low adsorption capacity and weak binding forces contribute to rapid breakthrough times.

To overcome these challenges and fully harness the potential of MOFs, future research directions should focus on material design, process optimization, and techno-economic analysis. Key priorities include the development of hybrid materials that combine chemisorption and physisorption, such as amine-functionalized hierarchical MOFs with mesoporous networks, to effectively address diffusion barriers while maintaining CO_2 affinity. Advanced synthesis techniques, including defect engineering and post-synthetic modification, can significantly enhance low-pressure capture efficiency in DAC and natural gas applications. Moreover, energy-efficient regeneration strategies that incorporate innovative temperature and pressure swing cycles, along with renewable energy sources, are crucial for cost reduction. Emphasizing low-pressure CO_2 applications, such as DAC and industrial waste management, aligns seamlessly with global decarbonization goals.

Data availability

There is no data for this Frontier article.

Author contributions

Runzhi Wei: writing – original draft. Tao Zhao: validation. Hui Xu: writing – review & editing. Junkuo Gao: supervision, writing – review & editing.

Conflicts of interest

The authors state that they have no known conflicting financial interests or personal ties that might have influenced the work presented in this study.

Acknowledgements

This work was supported by the National Natural Science Foundation of China (22378366).

References

- J. T. Jia, P. M. Bhatt, S. R. Tavares, E. Abou-Hamad, Y. Belmabkhout, H. Jiang, A. Mallick, P. T. Parvatkar, G. Maurin and M. Eddaoudi, *Angew. Chem., Int. Ed.*, 2024, **63**, e202318844.
- Y. L. Zhao, X. Zhang, M. Z. Li and J. R. Li, *Chem. Soc. Rev.*, 2024, **53**, 2056–2098.
- L. R. Li, H. S. Jung, J. W. Lee and Y. T. Kang, *Renewable Sustainable Energy Rev.*, 2022, **162**, 112441.
- T. Liu, Y. Wang, Y. Wu, W. Jiang, Y. Deng, Q. Li, C. Lan, Z. Zhao, L. Zhu, D. Yang, T. Noël and H. Xie, *Nat. Commun.*, 2024, **15**, 10920.
- B. Song, Y. H. Liang, Y. Zhou, L. Zhang, H. Li, N. X. Zhu, B. Z. Tang, D. Zhao and B. Liu, *J. Am. Chem. Soc.*, 2024, **146**, 14835–14843.
- R. Z. Wei, T. Alshahrani, B. L. Chen, A. B. Ibragimov, H. Xu and J. K. Gao, *Sep. Purif. Technol.*, 2025, **352**, 128238.
- S. Kumar, R. Muhammad, A. Amhamed and H. Oh, *Coord. Chem. Rev.*, 2025, **522**, 216230.
- P. Z. Moghadam, Y. G. Chung and R. Q. Snurr, *Nat. Energy*, 2024, **9**, 121–133.
- X. Wang, Y. Q. Chen, W. H. Li, C. Q. Wang, T. Zhao, A. B. Ibragimov and J. K. Gao, *Chem. Eng. J.*, 2024, **498**, 155338.
- Z. Zhou, T. Ma, H. Zhang, S. Chheda, H. Li, K. Wang, S. Ehrling, R. Giovine, C. Li, A. H. Alawadhi, M. M. Abduljawad, M. O. Alawad, L. Gagliardi, J. Sauer and O. M. Yaghi, *Nature*, 2024, **635**, 96–101.
- J. X. Wang, C. C. Liang, X. W. Gu, H. M. Wen, C. H. Jiang, B. Li, G. D. Qian and B. L. Chen, *J. Mater. Chem. A*, 2022, **10**, 17878–17916.
- Y. C. Zheng, Y. Q. Chen, J. J. Niu, T. Zhao, A. B. Ibragimov, H. Xu and J. K. Gao, *Sep. Purif. Technol.*, 2025, **354**, 128890.
- Z. Zhou, T. Ma, H. Zhang, S. Chheda, H. Li, K. Wang, S. Ehrling, R. Giovine, C. Li, A. H. Alawadhi, M. M. Abduljawad, M. O. Alawad, L. Gagliardi, J. Sauer and O. M. Yaghi, *Nature*, 2024, **635**, 96–101.
- K. Sun, Y. Y. Qian and H. L. Jiang, *Angew. Chem., Int. Ed.*, 2023, **62**, e202217565.
- F. Zheng, R. D. Chen, Z. X. Ding, Y. Liu, Z. G. Zhang, Q. W. Yang, Y. W. Yang, Q. L. Ren and Z. B. Bao, *J. Am. Chem. Soc.*, 2023, **145**, 19903–19911.
- X. Q. Zhu, T. Ke, J. Y. Zhou, Y. F. Song, Q. Q. Xu, Z. G. Zhang, Z. B. Bao, Y. W. Yang, Q. L. Ren and Q. W. Yang, *J. Am. Chem. Soc.*, 2023, **145**, 9254–9263.
- A. E. Amooghin, H. Sanaeepur, R. Luque, H. Garcia and B. L. Chen, *Chem. Soc. Rev.*, 2022, **51**, 7427–7508.
- C. N. Li, L. Liu, S. Liu, D. Q. Yuan, Q. Zhang and Z. B. Han, *Small*, 2024, 2405561, DOI: [10.1002/sml.202405561](https://doi.org/10.1002/sml.202405561).
- P. Z. Li, X. J. Wang, K. Zhang, A. Nalaparaju, R. Y. Zou, R. Q. Zou, J. W. Jiang and Y. L. Zhao, *Chem. Commun.*, 2014, **50**, 4683–4685.
- R. C. Rohde, K. M. Carsch, M. N. Dods, H. Z. H. Jiang, A. McIsaac, R. Klein and H. Kwon, *Science*, 2024, **386**, 814–819.
- Z. Niu, X. L. Cui, T. Pham, G. Verma, P. C. Lan, C. Shan, H. B. Xing, K. A. Forrest, S. Suepaul, B. Space, A. Nafady, A. M. Al-Enizi and S. Q. Ma, *Angew. Chem., Int. Ed.*, 2021, **60**, 5283–5288.
- J. Yin, J. Wang, M. Sun, Y. Yang, J. Lyu, L. Wang, X. Dong, C. Ye and H. Bao, *Nat. Commun.*, 2025, **16**, 370.
- H. T. Shi, R. Cao, H. J. Zhang, J. J. Yang, Y. L. Fu and J. P. Chen, *Adv. Funct. Mater.*, 2025, **35**, 245211.
- Y. J. Wan, Y. F. Miao, T. J. Qiu, D. K. Kong, Y. X. Wu, Q. N. Zhang, J. M. Shi, R. Q. Zhong and R. Q. Zou, *Nanomaterials*, 2021, **11**, 3348.
- D. S. Choi, D. W. Kim, D. W. Kang, M. J. Kang, Y. S. Chae and C. S. Hong, *J. Mater. Chem. A*, 2021, **9**, 21424–21428.
- P. Horcajada, F. Salles, S. Wuttke, T. Devic, D. Heurtaux, G. Maurin, A. Vimont, M. Daturi, O. David, E. Magnier, N. Stock, Y. Filinchuk, D. Popov, C. Riekkel, G. Férey and C. Serre, *J. Am. Chem. Soc.*, 2011, **133**, 17839–17847.
- J. H. Choe, H. Kim, H. R. Y. Yun, M. J. Kang, S. Park, S. M. Yu and C. S. Hong, *J. Am. Chem. Soc.*, 2023, **146**, 646–659.
- O. I. F. Chen, C. H. Liu, K. Y. Wang, E. Borrego-Marin, H. Z. Li, A. H. Alawadhi, J. A. R. Navarro and O. M. Yaghi, *J. Am. Chem. Soc.*, 2024, **146**, 2835–2844.
- H. Lyu, O. I. F. Chen, N. Hanikel, M. I. Hossain, R. W. Flaig, X. K. Pei, A. Amin, M. D. Doherty, R. K. Impastato, T. G. Glover, D. R. Moore and O. M. Yaghi, *J. Am. Chem. Soc.*, 2022, **144**, 2387–2396.
- J. H. Li, Y. W. Gan, J. X. Chen, R. B. Lin, Y. S. Yang, H. Wu, W. Zhou, B. L. Chen and X. M. Chen, *Angew. Chem., Int. Ed.*, 2024, **63**, e202400823.
- J. B. Lin, T. T. T. Nguyen, R. Vaidhyanathan, J. Burner, J. M. Taylor, H. Durekova and F. Akhtar, *Science*, 2021, **374**, 1464–1469.
- P. Singh, H. D. Singh, A. H. Menon and R. Vaidhyanathan, *Chem. Commun.*, 2023, **59**, 5559–5562.
- S. Q. Yang, R. Krishna, H. W. Chen, L. B. Li, L. Zhou, Y. F. An, F. Y. Zhang, Q. Zhang, Y. H. Zhang, W. Li, T. L. Hu and X. H. Bu, *J. Am. Chem. Soc.*, 2023, **145**, 13901–13911.
- L. G. Hu, W. H. Wu, L. Jiang, M. Hu, H. X. Zhu, L. Gong, J. H. Yang, D. H. Lin and K. Yang, *ACS Appl. Mater. Interfaces*, 2023, **15**, 43925–43932.
- X. L. Wang, M. Alzayer, A. J. Shih, S. Bose, H. M. Xie, S. M. Vornholt, C. D. Malliakas, H. Alhashem, F. Joodaki, S. Marzouk, G. C. Xiong, M. Del Campo, P. Le Magueres, F. Formalik, D. Sengupta, K. B. Idrees, K. K. Ma, Y. W. Chen, K. O. Kirlikovali, T. Islamoglu, K. W. Chapman, R. Q. Snurr and O. K. Farha, *J. Am. Chem. Soc.*, 2024, **146**, 3943–3954.
- R. Oktavian, R. Goeminne, L. T. Glasby, P. Song, R. Huynh, O. T. Qazvini, O. Ghaffari-Nik, N. Masoumifard, J. L. Cordiner, P. Hovington, V. Van Speybroeck and P. Z. Moghadam, *Nat. Commun.*, 2024, **15**, 3898.
- P. Nugent, Y. Belmabkhout, S. D. Burd, A. J. Cairns, R. Luebke, K. Forrest, T. Pham, S. Q. Ma, B. Space, L. Wojtas, M. Eddaoudi and M. J. Zaworotko, *Nature*, 2013, **495**, 80–84.

- 38 Y. Q. Hu, Y. J. Jiang, J. H. Li, L. Y. Wang, M. Steiner, R. F. Neumann, B. Q. Luan and Y. B. Zhang, *Adv. Funct. Mater.*, 2023, **33**, 2213915.
- 39 X. L. Cui, K. J. Chen, H. B. Xing, Q. W. Yang, R. Krishna, Z. B. Bao, H. Wu, W. Zhou, X. L. Dong, Y. Han, B. Li, Q. L. Ren, M. J. Zaworotko and B. L. Chen, *Science*, 2016, **353**, 141–144.
- 40 R. B. Lin, S. C. Xiang, W. Zhou and B. L. Chen, *Chem*, 2020, **6**, 337–363.
- 41 Y. Q. Zhang, L. Liu, W. Z. Li, B. H. Wu, C. N. Li, J. Q. Chu and Z. B. Han, *Inorg. Chem.*, 2024, **63**, 7705–7713.
- 42 H. N. Wamba, S. Dalakoti, N. Singh, S. Divekar, J. Ngoune, A. Arya and S. Dasgupta, *Ind. Eng. Chem. Res.*, 2023, **62**, 19773–19783.
- 43 I. A. Lázaro, E. C. Mazarakioti, E. Andres-Garcia, B. J. C. Vieira, J. C. Waerenborgh, I. J. Vitórica-Yrezábal, M. Giménez-Marqués and G. M. Espallargas, *J. Mater. Chem. A*, 2023, **11**, 5320–5327.
- 44 Y. S. Shi, Y. Xie, H. Cui, Z. A. Alothman, O. Alduhaish, R. B. Lin and B. L. Chen, *Chem. Eng. J.*, 2022, **446**, 137101.
- 45 Z. H. Qiao, S. Zhao, M. L. Sheng, J. X. Wang, S. C. Wang, Z. Wang, C. L. Zhong and M. D. Guiver, *Nat. Mater.*, 2019, **18**, 163–169.
- 46 J. M. Yuan, M. B. Gao, Z. Q. Liu, X. M. Tang, Y. Tian, G. Ma, M. Ye and A. M. Zheng, *Nat. Commun.*, 2023, **14**, 1735.
- 47 Y. C. Xiao, A. N. Hong, Y. C. Chen, H. J. Yang, Y. X. Wang, X. H. Bu and P. Y. Feng, *Small*, 2023, **19**, 2205119.
- 48 P. Z. Li, X. J. Wang, S. Y. Tan, C. Y. Ang, H. Z. Chen, J. Liu, R. Q. Zou and Y. L. Zhao, *Angew. Chem., Int. Ed.*, 2015, **54**, 12748–12752.